Robotic Cell Rotation Based on the Minimum Rotation Force

Qili Zhao, Mingzhu Sun, *Member, IEEE*, Maosheng Cui, Jin Yu, Yanding Qin, and Xin Zhao, *Member, IEEE*

***Abstract*—In this paper, a robotic cell rotation method based on the minimum rotation force is presented to adjust oocyte orientation in biological applications. In this method, the minimum rotation force, which can control the rotation angle (RA) of the oocyte quantitatively and generate minimum oocyte deformations, is derived through a force analysis on the oocyte in rotation. To exert this force on the oocyte, the moving trajectories (MT) of the injection micropipette (IM), are determined using mechanical properties of the oocytes. Further, by moving the IM along the designed MT, the rotation force control is achieved. To verify the feasibility of this method, a robotic rotation experiment for batch porcine oocytes are performed. Experimental results demonstrate that this system rotates the oocyte a10t an average speed of 28.6s/cell and with a success rate of 93.3%. More importantly, this method can generate much less oocyte deformations during cell rotation process compared with the manual method, while the average control error of RA in each step is only 1.2° (versus averagely 8.3° in manual operation), which demonstrates that our method can effectively reduce cell deformations and improve control accuracy of the RA.**

***Note to Practitioners*—Using an IM to rotate the oocyte is the most popular method to adjust oocyte orientations in many cellular biological applications. To rotate the oocyte precisely and reduce mechanical damages to the oocyte, the rotation force exerted on the oocyte should be estimated and controlled precisely. However, it is a challenging task and has not been resolved well. This paper calculates the minimum rotation force through the force analysis on oocyte and uses it to improve control accuracy of the RA and limit the cell deformations. Using calibrated oocyte mechanical properties, the MT of the IM corresponding to the minimum rotation force is designed. Then, by moving the IM along designed MT, the rotation force control is achieved online. This method does not rely on the force sensors and is realized on traditional micro-operation systems. Coupled with previous works, this method is able to operate batch oocytes one by one. Therefore, it can easily be applied in biological applications and replace manual operations.**

***Index Terms*—Cell mechanical properties, cell rotation, force control, micro-operation.**

Manuscript received February 04, 2014; revised June 23, 2014; accepted July 29, 2014. Date of publication October 28, 2014; date of current version October 02, 2015. This paper was recommended for publication by Associate Editor T. Kawahara and Editor Y. Sun upon evaluation of the reviewers' comments. This work was supported in part by the National Natural Science Foundation of China under Grant 61273341, Grant 61327802, and Grant 61105107, and in part by the National High-Tech Research Development Program (863 Program) under Grant 2013AA041102.

Q. L. Zhao, M. Z. Sun, J. Yu, Y. D. Qin, and X. Zhao are with the Institute of Robotics and Automatic Information System and the Tianjin Key Laboratory of Intelligent Robotics, Nankai University, Tianjin 300071, China (e-mail: zhaoxin@nankai.edu.cn).

M.S. Cui is with the Institute of Animal Sciences, Tianjin 300112, China.

This paper has supplementary downloadable multimedia material available at http://ieeexplore.ieee.org provided by the authors. The supplementary files contain three videos that display the global location of the batch oocytes, the automatic immobilization of the target oocyte, and the automatic rotation of oocyte. This material is 5.2 MB in size.

Color versions of one or more of the figures in this paper are available online at http://ieeexplore.ieee.org.

Digital Object Identifier 10.1109/TASE.2014.2360220

I. Introduction

CELL ROTATION, rotating some cellular structures (e.g., polar body) to a position desired for operation (e.g., 2 o'clock), is a requisite step in many cellular biological applications, such as nuclear transplantations (NT) [1], [2], embryo micro-injections [3], [4], and the polar-body biopsy [5]. At present, the cell rotation task is usually performed manually using the commercial micro-operation systems [6]. Taking the porcine oocyte rotation in the NT for example, the operator usually uses an injection micropipette (IM) to rotate the cell held by a holding micropipette (HM) gradually. First, the polar-body is moved to the focal plane from the initial position, which makes it visible. Then, the polar body is moved to the desired position in the focal plane such as two o'clock (see Fig. 1).

During above processes, the rotation force exerted on the oocyte by the IM should be controlled carefully. On one hand, the rotation force should be big enough to overcome the resistance force between the HM and the oocyte. If not, the slipping incidences between the IM and the oocyte occurs, which makes the rotation angle (RA) of the oocyte in each rotation step uncontrollable. On the other hand, the rotation force exerted on oocyte should be as small as possible, reducing mechanical damages to the oocyte development competence. Traditionally, the rotation forces are estimated and exerted on the oocyte manually during rotation process, which highly relies on the operating experiences. Hence, the manual rotation of the oocyte is a challenging task and should be performed by the operator with high professional skills. Certainly, the appropriate rotation force can be calibrated through sensors [7]–[10]. However, the calibrated results for one oocyte are not able to be used to rotate other oocytes because the mechanical properties of different oocytes vary significantly [11].

With the fast development of the robotics and automation techniques, a number of new noninvasive technologies have been used to adjust cell orientations. The dielectrophoresis (DEP) is able to use a nonuniform electric fields to rotate cells [12]–[15]. However, it is reported that the electric filed do great harm to cells [16]. The static magnetic field can generate a force on cells and has been used to adjust cell orientations [17], [18]. Using this method, the cells are only able to be oriented

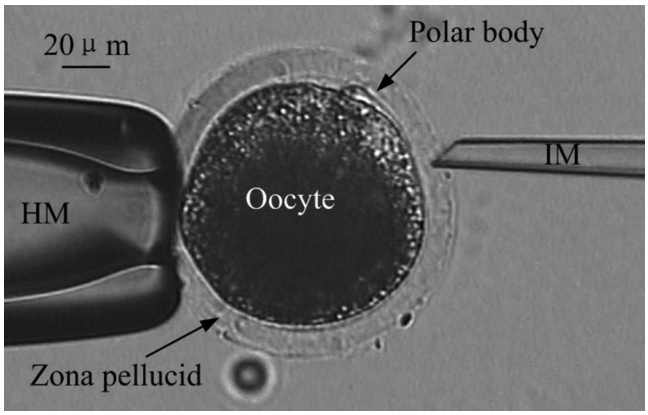

Fig. 1. Porcine oocyte rotation in nuclear transplantation.

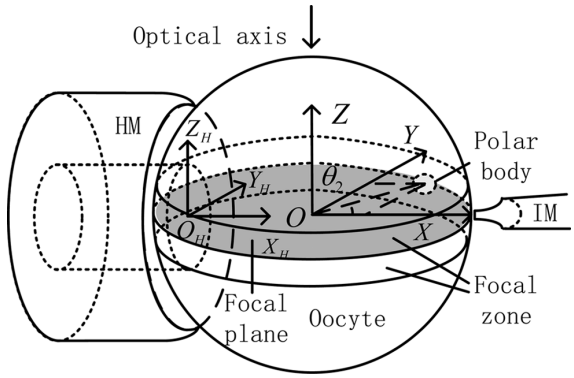

Fig. 2. Schematic: oocyte rotation.

to alignment with the magnetic field. Optical tweezers with a focused laser beam is able to exert a force on cells and rotate cells [19]–[22]. The customized rotational stage is also used to rotate the cells through an in-plane rotation movement [23]. However, the optical tweezers and rotation stage techniques can only rotate the cell about one axis [24], which cannot fulfill the 3-D rotation requirement in many biological applications, such as the NT. Recently, the micro-fluidics has been used to manipulate cells [25] and some researchers have realized a 3-D rotation of mouse embryos using micro-fluidic flow generated by HM [26]. However, as a noninvasive cell rotation method, the operator needs to immobilize the embryo/oocyte before performing the following operations (such as micro-injection and enucleation), which can change the cell orientation again. Different with the above methods relying on new devices, we presented a robotic 3-D rotation for the single cell using the traditional micro-operation system in previous studies [27]. As the MT of the IM in this method is derived through imitating manual operation, it usually cannot exert an appropriate rotation force on the cell. Hence, there are still relative large control errors of the RA in each step (with average control error of 7°).

As mentioned above, the rotation force is required to be as small as possible provided that it can overcome the resistance force. Therefore, the minimum rotation force meeting this requirement (the minimum rotation force) is the one which rotates the oocyte in an equilibrium state. As the oocyte is in an equilibrium state, the slipping incidences between the IM and the oocyte can be eliminated. Subsequently, the RA of each rotation step can be controlled quantitatively through the MT of the IM. Further, the oocyte in this state can be solidified and its balanced state will not be disturbed according to static theory. Hence, the minimum rotation force can be calculated through the analysis method used for the rigid body. Base on this point, a force analysis on oocyte in rotation process is performed to get the minimum rotation force. To exert this force on the cell, the oocyte mechanical properties, such as the Young's modulus of the zona pellucid (ZP), and friction coefficients between the oocyte and micropipettes, are calibrated and used to determine the corresponding MT of the IM. Further, traditional motion controllers are designed to achieve online rotation force control during rotation process. Finally, a robotic rotation experiment for batch oocytes is performed and the feasibility of this method is validated.

The remainder of this paper is organized as follows. In Section II, the derivation of the minimum rotation force using force analysis is introduced. Then, the MT of the IM for each oocyte based on the minimum rotation force is designed in Section III. After that, the control process of the rotation force is given in Section IV. Validation experiments on porcine oocytes are introduced in Section V and the conclusion is given in Section VI. The robotic calibration methods for oocyte mechanical properties are given in the Appendix.

II. The Derivation of the Minimum Rotation Force

Fig. 2 depicts the schematic of oocyte rotation. Due to the occlusion of the cytoplasm (which usually has a poor optical transparency), the polar body is visible only when it is moved into an area near the focal plane. This area is described as the "focal zone" in this paper. Define $O-XYZ$ as the cell rotation coordinate frame, where O is located at the cell center, X coincides with the central axis of the HM, and $X-Y$ plane coincides with the focal plane.

According to whether the polar body is visible or not, the oocyte rotation process is divided into two stages. In the first stage, the IM exerts a rotation force in the $X-Z$ plane, gradually moving the polar body to the focal zone from the initial position. In the second stage, the IM rotates the oocyte in the $X-Y$ plane. Step by step, the polar body is moved to the desired angular position in $X-Y$ plane, such as 2 o'clock.

As mentioned in the introduction part, the minimum rotation force can be calculated using methods in the static theory suited for a rigid body, such as the force analysis. Fig. 3(a) gives the schematic of the forces analysis to the oocyte in the first stage. The force exerted by IM, F_{I} , is divided into the poking force F_{In} along the normal direction and the rotation force $F_{\mathrm{I}\tau}$ along the tangential direction. They have a relationship as

$$F_{\mathrm{I}\tau} = F_{\mathrm{In}} \tan\alpha \tag{1}$$

$$F_{\mathrm{I}} = \sqrt{F_{\mathrm{I}\tau}^2 + F_{\mathrm{In}}^2} \tag{2}$$

where α is the angle between F_{In} and F_{I}.

The effects applied by the HM are divided into four parts: the suction force F_{H} along $-X$ axis; the supporting force F_{N} along X axis; the friction force F_{S}, which parallels with Y axis; and

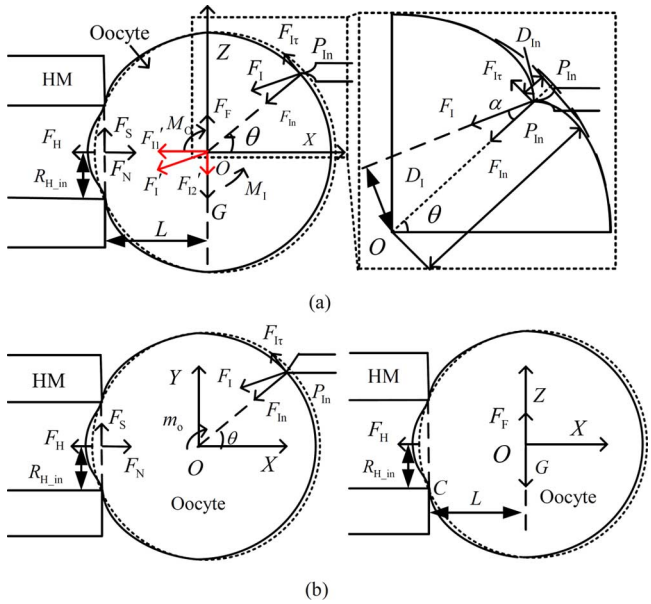

Fig. 3. Schematic: force analysis on oocyte in stage 2. (a) Force analysis on oocyte in stage 1. (b) Force analysis on oocyte in stage 2.

M_{O}, a couple balancing the moment of F_{I}. Here, F_{H} is defined as

$$F_{\mathrm{H}} = \pi R_{\mathrm{H\_in}}^2 {}^* P \tag{3}$$

where $R_{\mathrm{H\_in}}$ is the inner radius of the HM and P is the aspiration pressure.

Furthermore, gravity G and buoyancy F_{F} of the oocyte are also considered in the force analysis. They are separately expressed as

$$G = 4\pi R_0^3 \frac{\rho g}{3} \tag{4}$$

$$F_{\mathrm{F}} = 4\pi R_0^3 \frac{\rho_1 g}{3} \tag{5}$$

where ρ and ρ_1 are the densities of the oocyte and the culture medium, respectively, R_0 is the radius of the oocyte.

If the oocyte is in an equilibrium state, according to static theory, the affection of F_{I} can be replaced by force F_{I}' and a rotation moment M_{I} at O, where F_{I}' equals F_{I} and M_{I} can be determined as

$$M_{\mathrm{I}} = F_{\mathrm{I}} {}^* D_{\mathrm{I}} = F_{\mathrm{I}\tau} {}^* (R_0 - D_{\mathrm{In}}) \tag{6}$$

where D_{In} is the poking depth, as shown in Fig. 3.

Further, F_{I}' can be divided into two component forces at O : F_{I1}' and F_{I2}', where F_{I1}' and F_{I2}' are along with X axis and Z axis separately. According to geometrical relationships, they can be derived separately as

$$F_{\mathrm{I1}}' = F_{\mathrm{I}}' {}^* \cos(\theta - \alpha) = F_{\mathrm{In}} {}^* \frac{\cos(\theta - \alpha)}{\cos\alpha} \tag{7}$$

$$F_{\mathrm{I2}}' = F_{\mathrm{I}}' {}^* \sin(\theta - \alpha) = F_{\mathrm{In}} {}^* \frac{\sin(\theta - \alpha)}{\cos\alpha} \tag{8}$$

where θ is the angular position of the contact point between the IM and the cell.

As the forces and moments exerted on the oocyte keeps balanced, there are

$$F_{\mathrm{I1}}' = F_{\mathrm{N}} - F_{\mathrm{H}} \tag{9}$$

$$F_{\mathrm{I2}}' = F_{\mathrm{S}} + F_{\mathrm{F}} - G \tag{10}$$

$$M_0 = M_{\mathrm{I}} - F_{\mathrm{S}} {}^* L = F_{\mathrm{I}\tau} {}^* (R_0 - D_{\mathrm{In}}) - F_S {}^* L. \tag{11}$$

Substitute (1), (8), and (10) into (11), Mo can be calculated as

$$M_0 = F_{\mathrm{In}} {}^* (R - D_{\mathrm{In}})^* \tan\alpha - \left(\frac{F_{\mathrm{In}} {}^* \sin(\theta - \alpha)}{\cos\alpha} + G - F_{\mathrm{F}} \right) * L. \tag{12}$$

The maximum resistant moment M_{Hmax} provided by the HM is defined as

$$M_{\mathrm{H\,max}} = \mu_{\mathrm{H}} {}^* F_{\mathrm{N}} {}^* L + M_0 \tag{13}$$

where L is the distance from the tip of the HM to O, which can be estimated by

$$L = (R_0^2 - R_{\mathrm{H\_in}}^2)^{1/2}. \tag{14}$$

In order to rotate the oocyte around the central axis in an equilibrium state, M_{I} should be equal to $M_{\mathrm{H\,max}}$, which means

$$F_{\mathrm{I}\tau} {}^* (R_0 - D_{\mathrm{In}}) = \mu_{\mathrm{H}} {}^* F_{\mathrm{N}} {}^* L + M_{\mathrm{O}} \tag{15}$$

according to (6) and (13).

Substitute (1), (7), (9), and (12) into (15), the poking force F_{In} required by rotating the oocyte at a state of equilibrium in the first rotation stage can be derived as

$$F_{\mathrm{In}} = \frac{(\mu_{\mathrm{H}} F_{\mathrm{H}} + F_{\mathrm{F}} - G)\cos\alpha}{\sqrt{(1+\mu_{\mathrm{H}}^2)}\sin(\theta - \alpha - \arctan\mu_{\mathrm{H}})} \tag{16}$$

where μ_{H} is the friction coefficient between the HM and the oocyte.

The rotation force $F_{\mathrm{I}\tau}$ is generated by the poking force F_{In}, which is subsequently generated by the poking depth D_{In}. Increasing the D_{In} gradually and then moving the IM along the tangential direction of the cell surface, the maximum $F_{\mathrm{I}\tau}$ before the oocyte is rotated around can be calculated as

$$F_{\mathrm{I}\tau} = \mu_{\mathrm{I}} {}^* F_{\mathrm{In}} \tag{17}$$

where μ_{I} is the frictional coefficient between the IM and the oocyte. When the oocyte is just moved around, the derived F_{In} is the minimum one given in (16), therefore, the minimum mechanical damage to the oocyte is generated.

Substitute (1) and (16) into (17), the minimum rotation force $F_{\mathrm{I}\tau}$ can be calculated as

$$F_{\mathrm{I}\tau} = \frac{(\mu_{\mathrm{H}} F_{\mathrm{H}} + F_F - G)\mu_{\mathrm{I}}}{\sqrt{(1+\mu_{\mathrm{H}}^2)(1+\mu_{\mathrm{I}}^2)}\sin(\theta - \arctan\mu_{\mathrm{I}} - \arctan\mu_{\mathrm{H}})}. \tag{18}$$

As shown in Fig. 3(b), the force analysis of the oocyte in the second stage is similar to that in the first stage, except that F_{I} and F_{S} are all within the $X-Y$ plane instead of the $X-Z$ plane. Furthermore, in the second stage, the suction force F_{H} provides a compensating moment at the point C, the contacting point between the oocyte and the bottom inner surface of the

HM, keeping balance with the moment generated by G and F_{F} at C. The rotation force $F_{\mathrm{I}\tau}$ in the second stage can be obtained by

$$F_{\mathrm{I}\tau} = \frac{\mu_H \mu_{\mathrm{I}} (F_H + L^* \frac{(F_F - G)}{R_{H\_in}})}{\sqrt{(1+\mu_{\mathrm{H}}^2)(1+\mu_{\mathrm{I}}^2)}\sin(\theta - \arctan\mu_{\mathrm{I}} - \arctan\mu_{\mathrm{H}})}. \tag{19}$$

Combing (4), (5), (14), (18), and (19), it is not difficult to find that the bigger the oocyte is (with bigger R_0), the bigger minimum rotation force it needs. In our previous work, we measured that the average density of the oocyte is about $1.08 \times 10^3\ \mathrm{kg/m^3}$ [28]. The value of the μ_{H} is measured as more than 0.05 (see more details in Section III-B). The R_0 of the normal porcine oocyte is about 75–90 μm. The inner radius of the HM is about 30 μm. According to (14), L can be computed as 69–84.9 μm. Preliminary experiments demonstrate that the proper aspiration pressure in cell rotation is about 800 Pa. Using (3), F_{H} is estimated as more than 1.13×10^{-6}N. According to (4) and (5), $G - F_{\mathrm{F}}$ is about $1.5 \times 10^{-10} - 2.6 \times 10^{-10}$N, totally negligible compared with $\mu_{\mathrm{H}}{}^* F_{\mathrm{H}}$, which equals to 5.7×10^{-8}N. Moreover, the value of $L^*(G - F_{\mathrm{F}})/R_{\mathrm{H\_in}}$ is about $4.3 \times 10^{-10} - 7.4 \times 10^{-10}$N, which can be omitted compared with the value of F_{H}. Hence, (18) and (19) can be simplified as

$$F_{\mathrm{I}\tau} = \frac{\mu_{\mathrm{H}} \mu_{\mathrm{I}} F_{\mathrm{H}}}{\sqrt{(1+\mu_{\mathrm{H}}^2)(1+\mu_{\mathrm{I}}^2)}\sin(\theta - \arctan\mu_{\mathrm{I}} - \arctan\mu_{\mathrm{H}})}. \tag{20}$$

Using (17), the corresponding poking force F_{In} can be given as

$$F_{\mathrm{In}} = \frac{\mu_{\mathrm{H}} F_{\mathrm{H}}}{\sqrt{(1+\mu_{\mathrm{H}}^2)(1+\mu_{\mathrm{I}}^2)}\sin(\theta - \arctan\mu_{\mathrm{I}} - \arctan\mu_{\mathrm{H}})}. \tag{21}$$

Equation (20) gives the minimum rotation force which can rotate the oocyte with the minimum deformation and without slipping incidences in two stages.

According to (20), the effect of geometrical properties of the oocyte can be omitted. The minimum rotation force is mainly decided by the cell mechanical properties, such as the friction coefficients between the cell and the micropipettes.

III. Motion Trajectory Plan of the IM Using the Minimum Rotation Force

To exert the minimum rotation force on the oocyte, the MT plan of the IM is performed. As mentioned in Section II, the rotation force $F_{\mathrm{I}\tau}$ is generated by the poking force F_{In}, and F_{In} is determined by the poking depth of the IM, D_{In}, which supplies an approach to determine the MT of the IM through $F_{\mathrm{I}\tau}$. To achieve this, the relationship between F_{In} and D_{In} should be determined.

A. The Calibration of the Relationship Between the Poking Depth and Poking Force

This relationship between F_{In} and D_{In} is estimated using the biomembrane point-load model reported in [29] and [30]. According to this model, F_{In} can be estimated as

$$F_{\mathrm{In}} = K^* E^* \omega_{\mathrm{d}}^3 \tag{22}$$

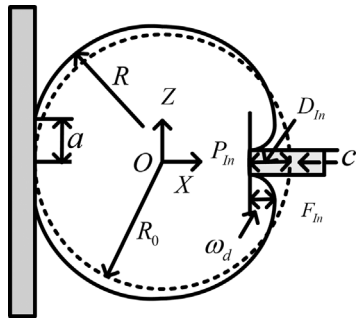

Fig. 4. Schematic: the biomembrane point-load model.

as shown in Fig. 4, where E is the Young's modulus of the zona pellucid (ZP), ω_{d} is the depth of the dimple created by F_{In}; and K can be derived by

$$K = \frac{2\pi h(3 - 4\xi^2 + \xi^4 + 2\ln\xi^2)}{a^2(1-v)(1-\xi^2)(1-\xi^2+\ln\xi^2)^3} \tag{23}$$

where a denotes the radius of the dimple, c denotes the radius of the IM and $\xi = c/a$, R represents the radius of the semicircular curved surface, and v denotes the Poisson's ratio which is traditionally set as 0.5.

As shown in Fig. 4, the poking depth can be obtained as follows:

$$D_{\mathrm{In}} = \omega_{\mathrm{d}} + 2(R_{\mathrm{O}} - R). \tag{24}$$

Sustitute (24) into (22), the relationship between D_{In} and F_{In} is expressed as

$$F_{In} = K^* E^* (D_{In} + 2(R - R_0))^3. \tag{25}$$

According to (25), this relationship between F_{In} and D_{In} is determined by E and deformation parameters of the oocyte during poking process, such as ω_{d}, R and a. According to the static theory, the deformation parameters are only determined by geometrical properties of the oocyte, such as oocyte size and ZP thickness, when using the same IM and HM. As oocytes in the experiments are previously selected to make sure that they have similar geometrical properties, the varying trend of their deformation parameters during poking process can be considered basically the same with each other. Hence, the only determining factor of the relationship between F_{In} and D_{In} is E, which needs to be measured for each oocyte. The poking experiment is only performed off line once for the first oocyte and the derived oocyte deformation parameters can be used to estimate the relationship of all remaining oocytes. According to (25), the harder the cell is, the less deformations (poking depth) required during rotation task.

To derive the relationship given in (25), the E and the oocyte deformation parameters of the first oocyte should be calibrated. The E is derived through a pneumatic micropipette aspiration operation, which is reported in [31]. To derive deformation parameters, a poking experiment is performed and introduced in the Appendix.

According to (21), θ should fulfill the condition as $\theta > \arctan\mu_{\mathrm{I}} + \arctan\mu_{\mathrm{H}}$. However, θ equals to zero in the biomembrane point-load model, as shown in Fig. 4, which

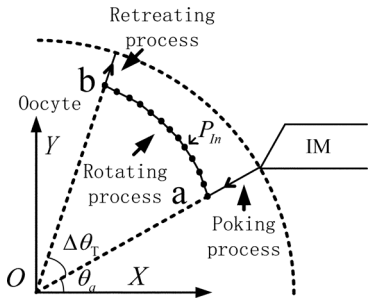

Fig. 5. Schematic: the rotation process of the IM in each rotation step.

is not the same case with that in the cell rotation process. Considering the offset of O is very small and the poking forces both pointing to O in two cases, this model is still used to estimate the relationship between $F_{\rm In}$ and $D_{\rm In}$ in the cell rotation process. Further, the feasibility of this assumption has been verified by the oocyte rotation results in Section VI. Moreover, to use the biomembrane point-load model, the slope IM used in this paper is carefully made to generate a flat tip with diameters of about 2–3 μm.

B. The Design of the Motion Trajectory of the IM

According to (25), the poking depth $D_{\rm In}$ is expressed as

$$D_{\rm In} = (\frac{F_{In}}{KE})^{1/3} + 2(R_0 - R). \tag{26}$$

The position of the contact point $P_{\rm In}$ is obtained by

$$P_{\rm In} = ((R_0 - D_{\rm In})^* \cos\theta, (R_0 - D_{\rm In})^* \sin\theta). \tag{27}$$

Series of $P_{\rm In}$ given in (27) make up the MT of the IM.

In order to exert the minimum rotation force at the beginning of each rotation step, the MT of the IM in each rotation step is departed into three processes (see Fig. 5): the poking process, the rotation process and the retreating process. In the poking process, the IM pokes into the oocyte surface at the depth given in (26). In the rotation process, the IM moves along the MT given in (27). In the retreating process, the IM leaves the cell surface along the normal direction. The RA in each step is controlled through the contacting angle between the MT and the oocyte, $\Delta\theta$, which is the central angle from the initial point a and ending point b in Fig. 5.

In order to determine the MT of the IM, $\mu_{\rm H}$ and $\mu_{\rm I}$ are required. The calibration of the two parameters is achieved through a rotation test which is introduced with details in the Appendix. As this experiment consumes lots of time, the calibration of $\mu_{\rm H}$ and $\mu_{\rm I}$ are not appropriate to be performed online for each oocyte. To resolve this problem, we derive ranges of $\mu_{\rm H}$ and $\mu_{\rm I}$ offline according to large numbers of experiments, and use them to design the MT of the IM.

According to preliminary experimental results, the varying ranges of $\mu_{\rm H}$ and $\mu_{\rm I}$ for different oocytes are $[0.040, 0.065]$ and $[0.11, 0.2]$, respectively. Under the appropriate aspiration pressure of 800 Pa, using (20), the relationships between $F_{{\rm I}\tau}$ and θ under different values of $(\mu_{\rm I}, \mu_{\rm H})$ are shown in Fig. 6. When $(\mu_{\rm I}, \mu_{\rm H})$ is set as $(0.2, 0.065)$, the maximum of the minimum rotation force is derived. This force can rotate different oocytes around and overcome the resistance force. Certainly, for the oocyte with

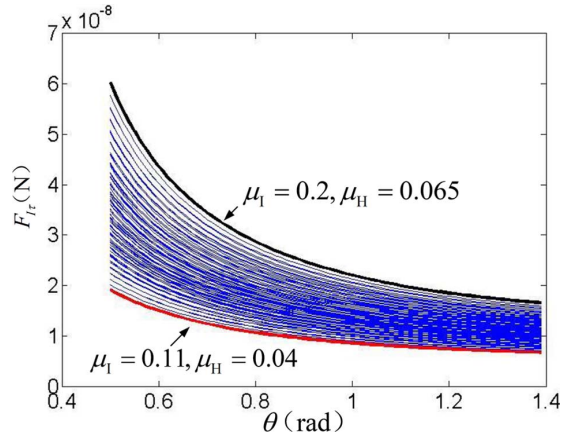

Fig. 6. The minimum rotation force under different frictional coefficients.

values of $(\mu_{\rm I}, \mu_{\rm H})$ other than $(0.2, 0.065)$, this force is larger than their minimum rotation force.

Setting $(\mu_{\rm I}, \mu_{\rm H})$ as (0.2, 0.065), the required $F_{\rm In}$ under different contact points can be derived according to (21). To prevent the penetration of the ZP and reduce the mechanical properties of the oocyte, the poking depth of the IM should be limited. In our experiments on mature porcine oocytes (incubated for two days) under the aspiration pressure of 800 Pa, the poking depth is limited under $0.25^* R_0$ (about 20 μm) to prevent the penetrations of the zona pellucid. According to the derived relationship between $F_{\rm In}$ and $D_{\rm In}$ in (25), the corresponding threshold poking force is about $1.2 \times 10^{-7} N$. Using (21), the minimum value of $\theta_{\rm a}$ is calculated as 0.9 rad. Further, to keep the oocyte in a balanced state, θ should be less than $\pi/2$ (1.57 rad).

Therefore, the feasible range of θ during the rotation process is $[0.9 \text{ rad}, 1.57 \text{ rad}]$ and $\theta_{\rm a}$ can be set as 0.9 rad. The maximum of $\Delta\theta$ is 0.67 rad, which is smaller than the value of RA (0.79 rad) making it possible for the polar body to pass over the focal zone in one rotation step [32]. Hence, $\Delta\theta$ is set as 0.67 rad in each step of the first stage until the polar body is detected visible. In the second stage, the polar body is visible. If the difference between angular position of the polar body, $\theta_{\rm P}$, and the desired angular position $\theta_{\rm D}$ is more than 0.67 rad, $\Delta\theta$ is set as 0.67 rad. Otherwise, $\Delta\theta$ is set as $|\theta_{\rm D} - \theta_{\rm p}|$.

IV. Rotation Force Control in Oocyte Rotation Process

In the poking process, the $F_{\rm In}$ needs to be controlled precisely according to (21). To eliminate the slipping incidences between the IM and oocyte, $F_{{\rm I}\tau}$ should be precisely controlled according to (20) in the rotation process. To achieve two above tasks, two kinds of motion controllers are developed to control the IM to move along derived MT of the IM.

In the first stage, the IM is at the position above the focal plane. Therefore, $P_{\rm In}$ is measured through encoders. In the second stage, as the IM is at a focused state, $P_{\rm In}$ is derived through image processing methods mentioned in the Appendix. Fig. 7 depicts the control block diagram for the oocyte rotation process.

In the poking process, the IM position in each sample period, $P_{\rm In}(i)$, is provided to system and the IM is moved to the point a

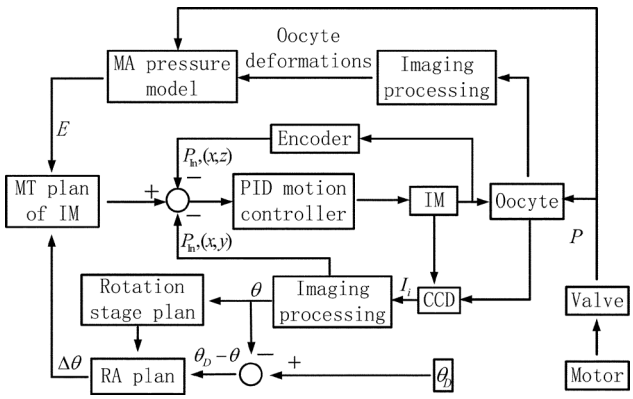

Fig. 7. The control block diagram of oocyte rotation process.

in Fig. 5. During this process, the moving speed of IM, $V_{\mathrm{In}}(i)$, is controlled as follows:

$$V_{\mathrm{In}}(i) = k_{\mathrm{P1}} {}^{*}(P_{\mathrm{a}} - P_{\mathrm{In}}(i)) + k_{\mathrm{I1}} {}^{*} \sum_{n=1}^{i}(P_{\mathrm{a}} - P_{\mathrm{In}}(i)) + k_{\mathrm{D1}} {}^{*}(P_{\mathrm{In}}(i-1) - P_{\mathrm{In}}(i)) \quad (28)$$

where k_{P1}, k_{I1}, and k_{D1} are proportion, integral, and derivative control gains, respectively; P_{a} is the position of point a. As P_{a} is a step input for this controller, the performance of the controller after a step input is used to adjust gain parameters. As the overshot of D_{In} may cause ZP penetration incidences, an overdamping configuration of gain parameters is selected. Through experiments, a configuration of $k_{\mathrm{P1}} = 4$, $k_{\mathrm{I1}} = 0.01$, and $k_{\mathrm{D1}} = 0.5$ is determined. Using (25), Fig. 8(a) gives the force control performance under a step input of this system. The steady-state error (about $2 \times 10^{-9} N$) is caused by the motion control error, which results from the image resolution of the microscopic image.

In the rotation process, the system divided the MT of the IM into series of IM position $P'_{\mathrm{In}}(\mathrm{i})$. Then, the designed moving speed of IM is determined as

$$V'_{\mathrm{In}}(i) = \frac{(P'_{\mathrm{In}}(i+1) - P'_{\mathrm{In}}(i))}{T} \quad (29)$$

where T is the control period of the system (0.05 s).

During rotation process, the moving speed of the IM is determined as

$$V_{\mathrm{In}}(i) = V'_{\mathrm{In}}(i) + k_{P2} {}^{*}(P'_{\mathrm{In}}(i) - P_{\mathrm{in}}(i)) + k_{I2} {}^{*} \sum_{k=1}^{i}(P'_{\mathrm{In}}(k) - P_{\mathrm{In}}(k)) + k_{D2} {}^{*}(P_{\mathrm{in}}(i-1) - P_{\mathrm{in}}(i)) \quad (30)$$

where k_{P2}, k_{I2}, and k_{D2} are the corresponding control gains, respectively.

Given designed MT, the $F_{\mathrm{I}\tau}$ in rotation process can be calculated online using (13) [see the calculated results in Fig. 8(b)]. In the rotation process, the control results of the $F_{\mathrm{I}\tau}$ can also be derived by (13). Testing results demonstrate that the average error between these two values is less than 5×10^{-10}N when $k_{\mathrm{P2}} = 0.1$, $k_{\mathrm{I2}} = 0.005$, and $k_{\mathrm{D2}} = 0.02$ [see Fig. 8(b)].

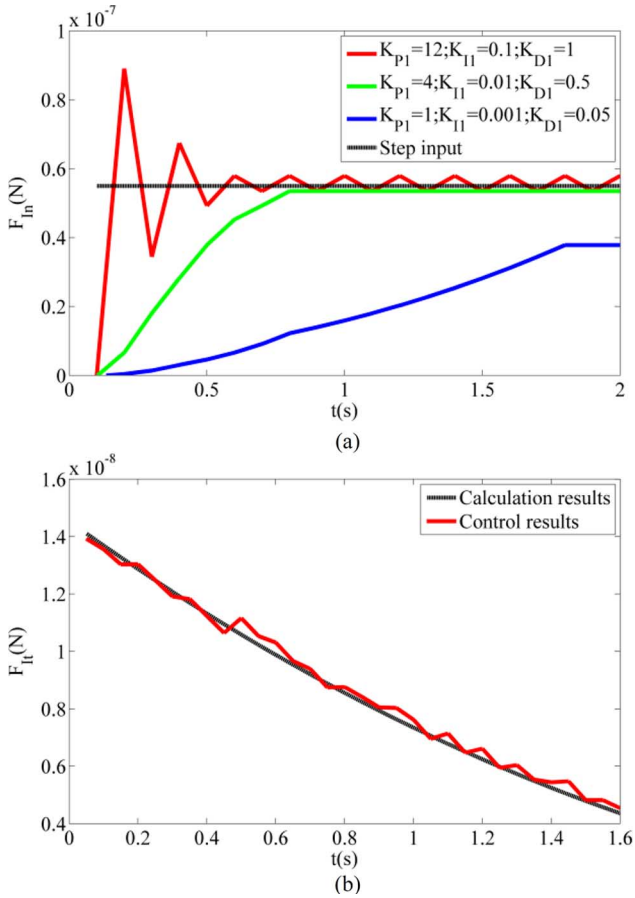

Fig. 8. Force control results. (a) Control results of F_{In} under different gain parameters. (b) Traction results for $F_{\mathrm{I}\tau}$ in rotation process.

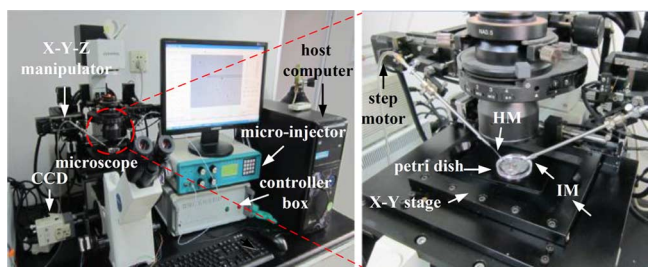

Fig. 9. The MR601 micro-operation system setup.

V. Experiments

A. System Setup

The designed oocyte rotation method is performed by the NK-MR601 micro-operation system [33]–[35], which is developed by our laboratory. The system setup is shown in Fig. 9. It consists of an inverted microscope (CK-40, Olympus); a CCD (W-V-460, Panasonic) for microscope image gathering at 30 frame/s; an in-house developed motorized X-Y stage (with a travel range of 100 mm, a maximum speed of 2 mm/s and a repeatability of ± 1 μm) for positioning cell samples which are placed in a 35 mm petri dish and covered by paraffin oil to prevent evaporation; a pair of X-Y-Z micromanipulators (with a travel range of 50 mm, a maximum speed of 1 mm/s and a repeatability of ± 1 μm) for positioning micropipettes; an inhouse developed pneumatic micro-injector supplying

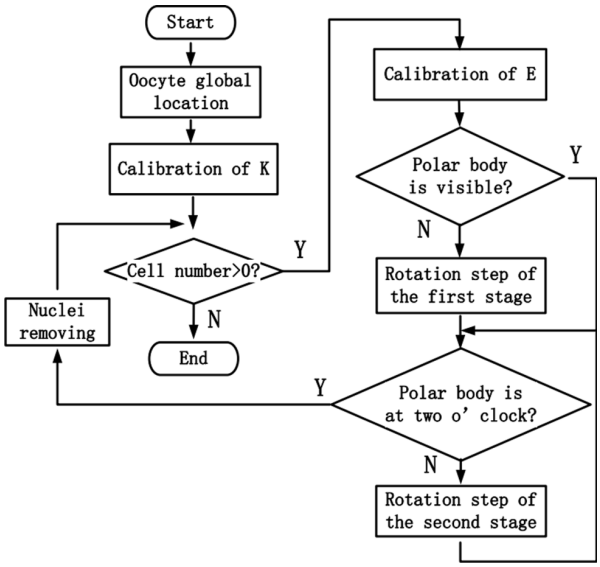

Fig. 10. The operation flow diagram of the robotic rotation process for batch oocytes.

negative aspiration pressure (with range of 0–3 kPa and resolution of 10 Pa) and positive injection pressure (with range of 0–200 kPa with resolution of 10 Pa); a host computer for microscopic image processing, pressure data acquisition and motion control of the platform and manipulators.

The IM is made from borosilicate glass tubes with outer diameter of 1 mm and inner diameter of 0.8 mm. The HM is made from borosilicate glass tubes with outer diameter of 1 mm and inner diameter of 0.6 mm. Both micropipettes are first pulled by a micropipette puller (MODEL P-97 Sutter Instrument) and then fractured by a micro-forge (MF-900 NARISHIGE) to generate the required out diameters (15–20 μm for the IM and 60–80 μm for the HM). After that, the opening of IM is first grinded by a micro-grinder (EG400 NARISHIGE) to generate a slope which is about 45° and then made by the micro-forge to generate a flat tip with diameter of about 2 μm. For the HM, it is melt on a micro-forge to make the opening smoothly and reduce its inner diameter to about 30 μm. Further, they are both bent 45° by the micro-forge and mounted on manipulators.

B. Experiments Process

In order to validate the feasibility of the oocyte rotation method presented in this paper, a robotic rotation for batch oocytes is performed using MR601 micro-operation system. In the experiment, a total number of sixty mature porcine oocytes are divided into three groups (20 oocytes in each group) to perform the cell rotation operation. After one group of oocytes are placed into the culture medium, a global location [33] for oocytes is performed to get their positions (see "1.avi" in the Supplementary Videos). And then, one by one, each oocyte is moved to the field of the view and immobilized by the HM automatically [34] (see "2.avi" in the Supplementary Videos).

Before rotation, the ZP Young's modulus of each oocyte is calibrated (see the Appendix). For the first oocyte, a poking experiment is performed to get the deformation parameters (see the Appendix) and derive the relationship between F_{In} and D_{In}. Then, an automated polar body recognition method [34] is performed to judge the initial position of the polar body. If the polar body is invisible, the first stage is performed; otherwise, the second stage is executed directly. Using previously derived oocyte property parameters, the MT of the IM in each rotation step is designed. Then, motion controllers move IM along the designed trajectories to rotate the oocyte gradually (see "3.avi" in the Supplementary Videos).

Fig. 10 gives the operation flow of the robotic rotation process for batch oocytes and Fig. 11 gives the rotation process on one oocyte.

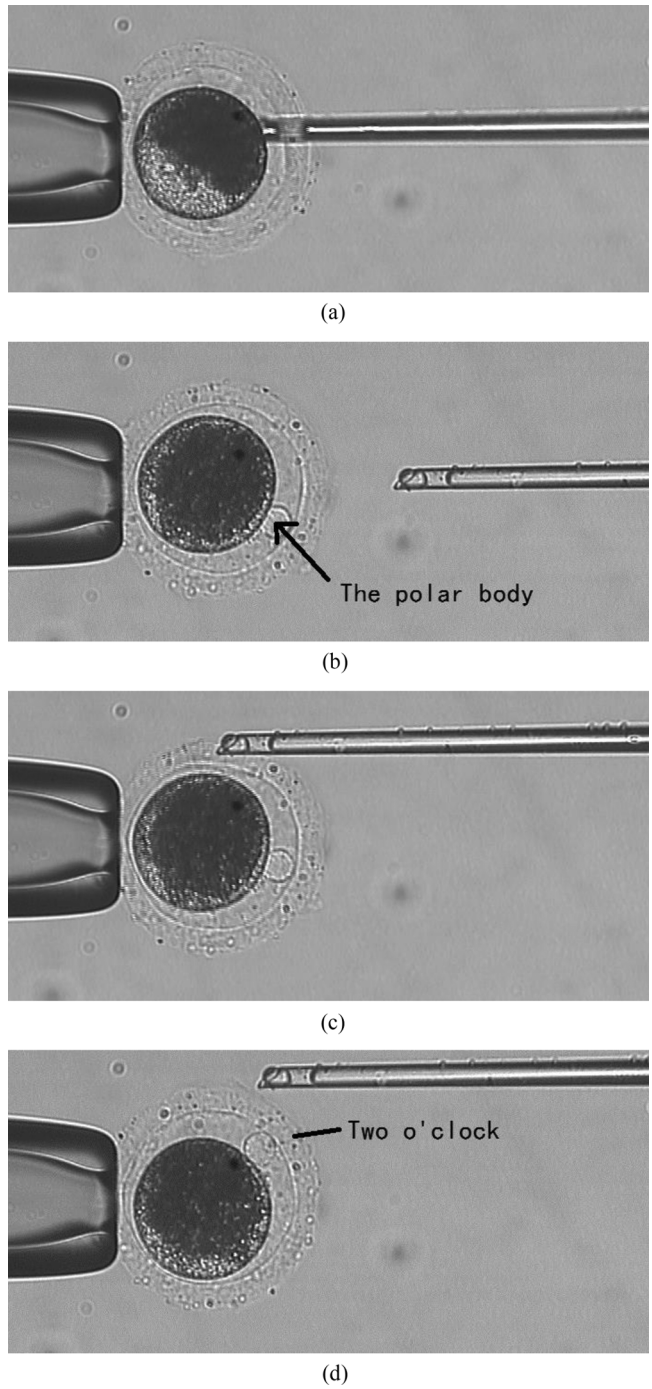

Fig. 11. The cell rotation process (see more details in the"3.avi" in the Supplementary Videos). (a) The first stage. (b) The results after the first stage. (c) The second stage. (d) The results after the second stage.

C. Experimental Results and Discussions

1) Oocyte Rotation Results: In the first stage, 59 of 60 oocytes are moved to the focal zone. One oocyte has an apparent elliptical shape which makes our method cannot provide enough rotation force to move the polar body into the focal zone. Hence, the success rate of the first stage is 98.3% (59 of 60). In the second stage, 56 oocytes are successfully operated and their polar bodies are moved to the desired angular position. The success rate of second rotation stage is 94.9% (56 of 59). Three failures cases happen when their polar bodies are abnormally small and moved out of the focal zone in the second stage. Therefore, the total success rate of our method is 93.3% (56 of 60). By comparison, reference [26] uses a fluidic flow to rotate the mouse embryos. The success rate of their method is 90%.

To get the average operation speed of our method, the operation time of 20 oocytes are derived. The four subtasks of the proposed oocyte rotation method: oocyte immobilization, Young's modulus detection, first rotation stage and second rotation stage, are 2.6, 16, 4.2, and 5.8 s, respectively. So, the average oocyte rotation speed of our method is 28.6 s/oocyte, which is 5.8 s longer than that of method in [26].

It is worthy to note that the operation time of the proposed method can be reduced significantly if the Young's modulus detection process, which costs about 16 s, is eliminated. As a matter of fact, this process will be not required anymore when the range of the Young's modulus for porcine oocytes is derived through testing large number of oocytes. Hence, the average operation time of our method may be reduced to about 12.6 s in the future. At present, our method is still faster than manual operation in our experiments (32.6 s). Further, our method is able to operate batch oocytes, which is vital for applications in many batch biological manipulations, such as NT.

2) RA Control Experiments: In order to test the control accuracy of RA in each step, ten oocytes are rotated with different $\Delta\theta$ in the second stage. For each oocyte, the $\Delta\theta$ varies from 10° (0.087 rad) to 35° (0.611 rad) with an interval of 5°. Under each $\Delta\theta$, the oocyte is rotated for six times and the average value of variation of angular position of the polar body, $\Delta\theta_{\mathrm{P}}$, is measured to quantify the RA. As a comparison, manual operations under the same conditions are performed by a high professional operator.

Fig. 12(a) and (b) give the $\Delta\theta_{\mathrm{P}}$ of one oocyte under different $\Delta\theta$ by two methods. It can be found that the differences between $\Delta\theta$ and $\Delta\theta_{\mathrm{P}}$ in our method are much smaller than those of manual operation. Subsequently, averaging the value of $\Delta\theta - \theta_{\mathrm{P}}$ under different $\Delta\theta$ as the control errors of RA, the derived results of ten oocytes are given in Fig. 12(c). It can be found that the control error of RA for every oocyte is significantly smaller than those of manual method. The average control error of RA for ten oocytes in our method is 1.2°, while that of the manual method is 8.3°.

The above experimental results demonstrate that our method effectively improves the control accuracy of RA. The control errors of our method are mainly caused by the assumption in determining relationship between D_{In} and F_{In}, and using a constant value of (μ_{I}, μ_{H}) to calculate MT of the IM.

Fig. 13 gives the generated D_{In} in a robotic and a manual rotation step when $\Delta\theta$ is set as 35° (0.611 rad). From Fig. 13,

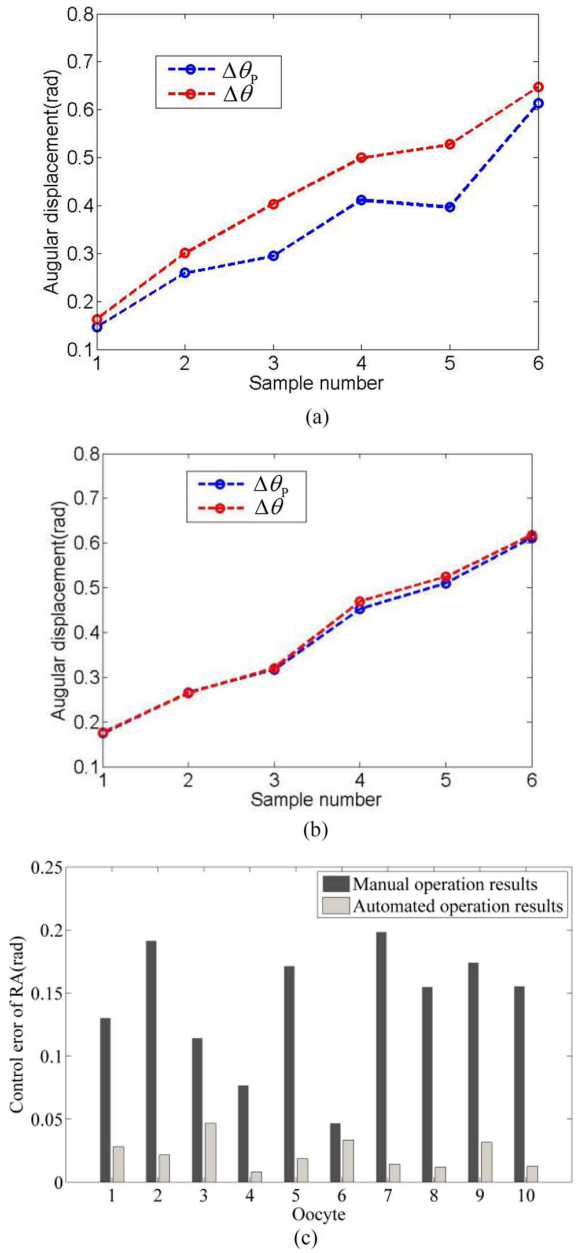

Fig. 12. The results of RA control experiment. (a) The value of $\Delta\theta_{\mathrm{P}}$ under $\Delta\theta$ in manual operation method. (b) The value of $\Delta\theta_{\mathrm{P}}$ under $\Delta\theta$ in our method. (c) The control error of RA for ten oocytes.

the average value of D_{In} generated in our method (with average value of 11.7 μm) is about 0.42-folded of that in the manual method (with average value of 28.2 μm). This result shows that our method can generate much less cell deformations in rotation process, which is very helpful to reduce mechanical damages to the oocyte development competence. This is mainly because the MT of the IM in our method is determined according to the minimum rotation force, while the one in manual operation is determined according to the operation experiences and is easily to be influenced by random factors.

VI. Conclusion

This paper proposes a novel oocyte rotation method based on the minimum rotation force. In this method, the minimum rotation force, which can rotate the oocyte quantitatively and gen-

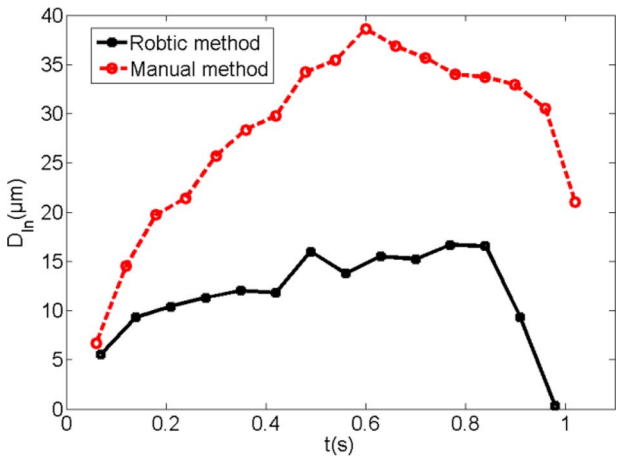

Fig. 13. The poking depth in a rotation step.

erate minimum rotation deformation, are calculated and used to perform robotic rotation for the oocyte.

Experimental results demonstrate that our method can rotate the oocyte with success rate of 93.3% at an operation speed of 28.6 s/oocyte. This operation speed can be further improved to about 12.6 s/oocyte by canceling the Young's modulus detection process when the range of Young's modulus of the porcine oocytes is derived. More importantly, the control error of the RA in each rotation step is 1.2°, which is apparently small than that of manual method (8.3°). At the same time, cell deformations generated in our method is only about 40% of that in manual method.

Compared with the manual cell rotation method, our method generates less cell deformations, has higher control accuracy and lower requirement for operators' working experiences. As our method is able to perform cell rotation on traditional micro-operation system using the common IM and HM, it can be directly used as the preoperation of the biological applications requiring adjusting cell orientations. Further, our method is able to operate batch oocytes, which will make our method used in the biological operations for batch oocytes.

After adjusting the maximum poking depth and the aspiration pressure according to the mechanical properties of other cells, the proposed method can be applied to the rotation of other spherical mammalian oocytes or embryos other than porcine oocytes.

APPENDIX
CALIBRATION PROCESS OF MECHANICAL PROPERTIES OF OOCYTE

As mentioned before, the oocyte mechanical property parameters are required to determine the MT of the IM, such as the ZP Young's modulus, the relationship between D_{In} and F_{In}, μ_{H} and μ_{I}. In these parameters, E is derived through a robotic micropipette aspiration (MA) method [31]. The relationship between D_{In} and F_{In} is calibrated through a poking experiment. Frictional coefficients μ_{H} and μ_{I} are derived through a rotation test.

Robotic Measurement of ZP Young's Modulus:

After each oocyte has been immobilized, the aspiration pressure increases from 0 to 1600 Pa with an interval of 200 Pa. During this process, a robotic pneumatic MA operation is performed to measure its Young's modulus. This MA process has been introduced in details in [31] and will not be reintroduced here. After that the measurement of E, the aspiration pressure is reduced to 800 Pa immediately for oocyte rotation.

The average measurement time for each oocyte is about 16 s. This process is mainly performed during the immobilized oocyte is moving to the appropriate operation area, and the IM is in preparation to rotate the oocyte. Hence, it will not take extra operation time in the cell rotation process.

Calibration of the Relationship Between the Poking Depth and Poking Force:

The relationship between F_{In} and D_{In} is calibrated through a poking experiment. After the oocyte is immobilized by the HM, the IM is moved to the position pointing to the center of the cell in Y direction and pokes into the surface of the oocyte with a speed of 10 $\mu\mathrm{m/s}$. During this process, oocyte deformation parameters are derived online through image processing methods. Subsequently, the relationship between F_{In} and D_{In} is calculated according to (24) and (25).

Before the poking experiment, a contour detection algorithm [28] is performed to get the radius of the target oocyte. During experiments, the P_{In} is derived indirectly through the positions of the gas-liquid-interface (GLI) P_{GLI}[32] [see Fig. 14(a)], which keeps a constant distance with P_{In} and can easily be derived by simple image processing methods. The position of the HM, P_{Ho}, is derived trough a template matching method [35]. Moreover, ω_{d} and a are derived, as shown in Fig. 14(b) as follows.

First, the microscopic picture is first convolved with a low-pass Gaussian filter to suppress the involved noises. Then, the obtained image is binarized by an Otsu adaptive thresholding method. After that, searching by column at P_{H}, a is determined. At the same time, the most right point of the oocyte, P_{MR}, is obtained through searching by row in two rectangular areas next to P_{In}. Subsequently, ω_{d} is derived by the distance between P_{In} and P_{MR}. Further, R is determined by the half of the distance between P_{In} and P_{Ho} in the X direction. Using (25), the relationship between F_{In} and D_{In} is quantified [see Fig. 14(c)].

Fig. 14(c) shows the obtained relationship between F_{In} and D_{In} for an oocyte with ZP Young's modulus of 16 Kpa. A fourth-order polynomial is chosen to fit the relationship between F_{In} and D_{In}. The fitted result shows that the relationship between F_{In} and D_{In} is nonlinear, which is in accordance with those reported in poking experiments on mouse embryos [29] and zebra fish embryos [36].

Estimation of the Friction Coefficients:

To derive the μ_{H} and μ_{I}, rotation tests are performed to derive several pairs of (θ, F_{In}) and use them to recognize (μ_{H}, μ_{I}) according to (21).

As mentioned in Section III, at each contact point with angular position θ, by increasing the poking depth D_{In} gradually and moving the IM along the tangential direction of the oocyte surface to rotate the oocyte, there exists a minimum poking

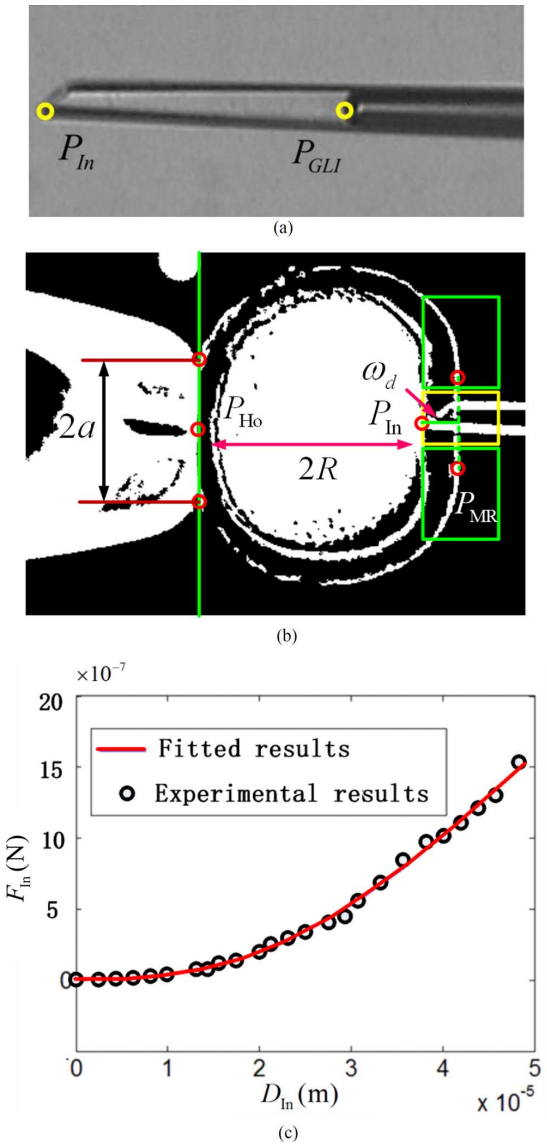

Fig. 14. Calibration of the relationship between F_{In} and D_{In} by the poking experiments. (a) The derivation of the P_{In}. (b) Calculation of the deformation parameters. (c) Calibrated relationship between F_{In} and D_{In}.

depth D_{In} which can just rotate the oocyte around the central axis without slipping incidences. (see Fig. 15).

As shown in Fig. 15(a), the poking depth is determined as

$$D_{\mathrm{In}} = R_0 - |P_{\mathrm{In}} - P_{\mathrm{O}}| \tag{31}$$

where P_{O} is the position of O. After each rotation step, the angular position of the polar body θ_{P} is detected through the image processing method [34]. The variation of θ_{P} in each step is used to estimate the RA in each rotation step. If the RA is detected more than 2° after a rotation step, the oocyte is considered to have been moved around and the corresponding D_{In} is derived according to (31). Then, according to the derived relationship between F_{In} and D_{In}, the corresponding threshold poking force F_{In} is calculated.

In order to reduce the calculation error of F_{In} caused by image processing in a rotation test, four pairs of derived (θ, F_{In})

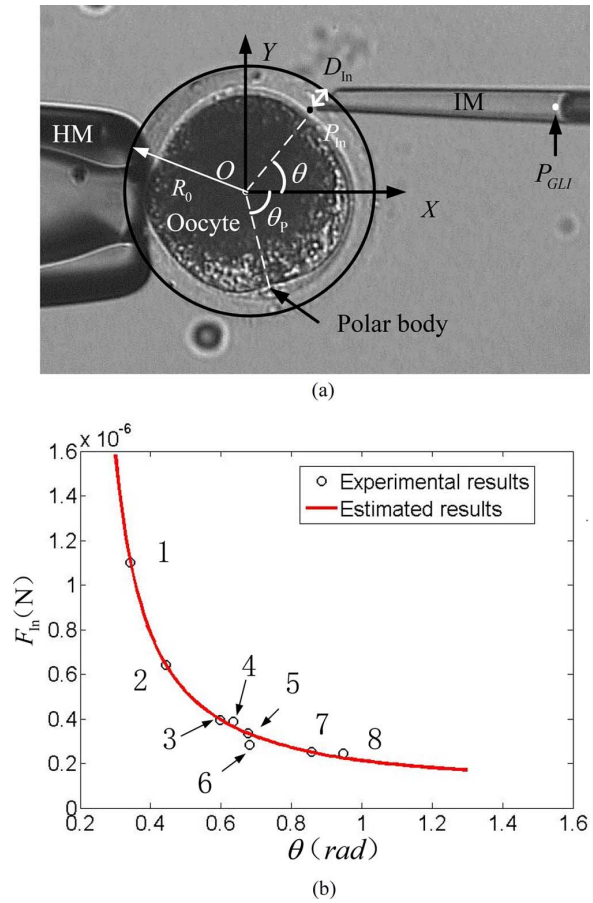

Fig. 15. Estimation of friction coefficients. (a) Image processing results in rotation results.(b) Estimation results and experimental results of F_{In}.

are used to estimate the (μ_{H}, μ_{I}) according to the least square method. Fig. 15(b) gives estimated relationship between F_{In} and θ by four pairs of (θ, F_{In}) (1, 3, 5, and 7). The remaining four pairs of detected results (2, 4, 6, and 8) are used to validate the estimated results. It can be found that the estimated relationship matches well with the rest of four pairs of (θ, F_{In}) (with average error less than 5%), which proves the feasibility of the estimated result.

It is worthy to note that, although the appropriate aspiration pressure in oocyte rotation operations is 800 Pa, it is not appropriate to be used in rotation test. Under this pressure, the derived D_{In} is usually too small to be precisely derived through image processing method. The aspiration pressure in rotation test is set as 1600 Pa.

REFERENCES

[1] I. Wilmut *et al.*, "Somatic cell nuclear transfer," *Nature*, vol. 10, no. 419, pp. 583–587, 2002.
[2] M. Tachibana *et al.*, "Human embryonic stem cells derived by somatic cell nuclear transfer," *Cell*, vol. 153, pp. 1228–1238, 2013.
[3] Z. Lu, X. P. Zhang, C. Leung, N. Esfandiari, R. F. Casper, and Y. Sun, "Robotic ICSI (Intracytoplasmic sperm injection)," *IEEE Trans. Biomed. Eng.*, vol. 58, no. 7, pp. 2102–2108, Jul. 2011.
[4] P. Stein and R. M. Schultz, "ICSI in mouse," *Methods Enzymol*, vol. 476, pp. 251–262, 2010.
[5] L. Gianaroli, "Preimplantation genetic diagnosis: Polar body and embryo biopsy," *Hum. Reprod.*, vol. 15, no. 4, pp. 69–75, 2000.
[6] [Online]. Available: http://www.eppendorf.com, www.narishige.co. jp, www.ais2.com

[7] R. J. Chang, C. C. Shiu, and C. Y. Cheng, "Self-biased-SMA drive PU microgripper with force sensing in visual servo," *Int. J. Adv. Robot. Syst.*, vol. 10, no. 280, pp. 1–12, 2013.
[8] H. B. Huang, D. Sun, J. K. Mills, W. J. Li, and S. H. Cheng, "Visual-based impedance control of out-of-plane cell injection systems," *IEEE Trans. Autom. Sci. Eng.*, vol. 6, no. 3, pp. 565–571, Jul. 2009.
[9] A. Pillarisetti, M. Pekarev, A. D. Brooks, and J. P. Desai, "Evaluating the effect of force feedback in cell injection," *IEEE Trans. Autom. Sci. Eng.*, vol. 4, no. 3, pp. 322–331, Jul. 2007.
[10] Z. Lu, C. Y. Chen, J. Nam, R. Ge, and W. Lin, "A micromanipulation system with dynamic force-feedback for automatic batch microinjection," *J. Micromech. Microeng.*, vol. 17, pp. 314–321, 2007.
[11] M. Khalilian *et al.*, "Estimating Young's modulus of zona pellucida by micropipette aspiration in combination with theoretical models of ovum," *J. R. Soc. Interface*, vol. 7, pp. 687–694, 2009.
[12] P. Benhal, J. G. Chase, P. Gaynor, B. Oback, and W. H. Wang, "AC electric field induced dipole-based on-chip 3D cell rotation," *Lab on Chip*, 2014, DOI:10.1039/C4LC00312H.
[13] L. H. Chau1, W. F. Liang, F. W. K. Cheung, W. K. Liu, W. J. Li, S. C. Chen, and G. B. Lee, "Self-rotation of cells in an irrotational AC E-field in an opto-electrokinetics chip," *Plos One*, vol. 8, no. 1, p. 51577, 2013.
[14] R. Kunikata, Y. Takahashi, M. Koide, T. Itayama, T. Yasukawa, H. Shiku, and T. Matsue, "Three dimensional microelectrode array device integrating multi-channel microfluidics to realize manipulation and characterization of enzyme-immobilized polystyrene beads," *Sens. Actuators B, Chem.*, vol. 141, no. 1, pp. 256–262, 2009.
[15] J. Park, S. W. Jung, Y. H. Kim, B. Kim, S. K. Lee, B. Ju, and K. I. Lee, "An integrated bio cell processor for single embryo cell manipulation," in *Proc. IEEE RSJ Int. Conf. Intell. Robots Syst.*, Sendai, Japan, 2004, pp. 242–247.
[16] D. S. Gray, J. L. Tan, J. Voldman, and C. S. Chen, "Dielectrophoretic registration of living cells to a microelectrode array," *Biosens. Bioelectron.*, vol. 19, no. 7, pp. 771–780, 2004.
[17] S. Schuerle, S. Erni, M. Flink, B. E. Kratochvil, and B. J. Nelson, "Three-dimensional magnetic manipulation of micro-and nanostructures for applications in life sciences," *IEEE Trans. Magn.*, vol. 49, no. 1, pp. 321–330, Jan. 2013.
[18] M. Ogiue-Ikeda and S. Ueno, "Magnetic cell orientation depending on celltype and cell density," *IEEE Trans. Magn.*, vol. 40, no. 4, pp. 3024–3026, Jul. 2004.
[19] C. Wang, S. Chowdhury, S. K. Gupta, and W. Losert, "Optical micromanipulation of active cells with minimal perturbations: direct and indirect pushing," *J. Biomed. Opt.*, vol. 18, no. 4, pp. 045001–045001.
[20] S. Bayoudh, T. A. Nieminen, N. R. Heckenberg, and H. Rubinsztein-Dunlop, "Orientation of biological cells using plane-polarized Gaussian beam optical tweezers," *J. Mod. Opt.*, vol. 50, no. 10, pp. 1581–1590, 2003.
[21] M. Ichikawa, K. Kubo, K. Yoshikawa, and Y. Kimura, "Tilt control in optical tweezers," *J. Biomed. Opt.*, vol. 13, no. 1, p. 101503, 2008.
[22] Y. L. Liang, Y. P. Huang, Y. S. Lu, M. T. Hou, and J. A. Yeh, "Cell rotation using optoelectronic tweezers," *Biomicrofluidics*, vol. 4, no. 4, 2010.
[23] M. C. Wu, "Optoelectronic tweezers," *Nat. Photon.*, vol. 5, pp. 322–324, 2011.
[24] X. Liu, Z. Lu, and Y. Sun, "Orientation control of biological cells under inverted microscopy," *IEEE/ASME Trans. Mechatron.*, vol. 16, no. 5, pp. 918–924, Oct. 2011.
[25] H. Yun, K. Kim, and W. G. Lee, "Cell manipulation in microfluidics," *Biofabrication*, vol. 5, pp. 1–14, 2013.
[26] C. Leung, Z. Lu, X. P. Zhang, and Y. Sun, "Three-dimensional rotation of mouse embryos," *IEEE Trans. Biomed. Eng*, vol. 59, no. 4, pp. 1049–1056, Apr. 2012.
[27] Q. L. Zhao, X. Zhao, Y. L. Wang, M. Z. Sun, M. S. Cui, J. Z. Feng, and G. Z. Lu, "Research on autonomous movement of oocyte in nuclei transplantation," *Control Eng. China* vol. 19, pp. 389–393, 2012 [Online]. Available: http://www.cnki.com.cn/Article/CJFD-Total-JZDF201203006.htm
[28] Q. L. Zhao, M. Z. Sun, M. S. Cui, J. Yu, and X. Zhao, "Robotic weighing for spherical cells based on falling speed detection," *Proc.3-M NANO*, pp. 264–268, 2013.
[29] Y. Sun, K. T. Wan, K. P. Roberts, J. C. Bischof, and B. J. Nelson, "Mechanical property characterization of mouse zona pellucida," *IEEE Trans. Nanobiosci.*, vol. 2, pp. 279–286, Dec. 2003.
[30] M. Ammi and A. Ferreira, "Realistic visual and haptic rendering for biological-cell injection," in *Proc. IEEE Int. Conf. Robot. Autom.*, 2005, pp. 918–923.
[31] Q. L. Zhao, M. Wu, M. S. Cui, Y. D. Qin, J. Yu, M. Z. Sun, X. Zhao, and X. Z. Feng, "A novel pneumatic micropipette aspiration method using a balance pressure model," *Rev. Sci. Instruments*, vol. 84, p. 123703, 2013.
[32] Q. L. Zhao, M. S. Cui, M. Z. Sun, Y. D. Qin, and X. Zhao, "A cell rotation method based on the kinematics model," *Robot*.
[33] Q. L. Zhao, M. S. Cui, X. Zhao, and M. Z. Sun, "Batch-operation process of nuclear transplantation based on global field of view," in *Proc. CCC Int. Conf.*, Yantai, China, Jul. 2011, pp. 4089–4094.
[34] Q. L. Zhao, M. S. Cui, C. Y. Zhang, J. Yu, M. Z. Sun, and X. Zhao, "Robotic enucleation for oocytes," in *Proc. IEEE NEMS Int. Conf.*, Waikili Beach, HI, USA, 2014, pp. 23–27.
[35] Y. L. Wang, X. Zhao, Q. L. Zhao, M. Z. Sun, and G. Z. Lu, "Automatic somatic cell operating process for nuclear transplantation," in *Proc. NEMS*, 2012, pp. 359–363.
[36] Y. H. Tan, D. Sun, W. H. Huang, and S. H. Cheng, "Mechanical modeling of biological cells in microinjection," *IEEE Trans. Nanobiosci.*, vol. 7, no. 4, pp. 257–266, Dec. 2008.

Qili Zhao received the B.Eng. degree in automation from Shandong Univerisity of Science and Technology, Tsingdao, China, in 2008, and the Ph.D. degree in control theory and control engineering from Nankai University, Tianjin, China in 2014.

He is a Postdoctoral Researcher with the Robotics and Mechatronics Research Laboratory, Department of Mechanical and Aerospace Engineering, Monash University, Clayton, Australia. His research interests include micro-characterization of biological cells, micro-robotic manipulation of biological cells, and micro-fluidics for biological applications.

Mingzhu Sun (M'12) received the B.S., M.S., and Ph.D. degrees in computer science and technology, computer application, control theory and control engineering from Nankai University, Tianjin, China, in 2003, 2006, and 2009, respectively.

Since 2009, she has been with the Institute of Robotics and Automatic Information System and the Department of Automation and Intelligence Science, Nankai University, Tianjin, China, as a Lecturer. Her research interests are in micro-manipulator for life science, image processing and computer vision.

Maosheng Cui received the B.A. degree from the Department of Animal Science, AnHui Technologic College, Hefei, China, in 2003, the M.A. degree from the Animal Science College of Yunnan Agricultural University, Yunnan, China, in 2006, and the Ph.D. degree from the Animal Science College of the Chinese Agricultural University, Beijing, China.

He was a Postdoctoral Researcher with the Chinese Academic of Agricultural Sciences from 2011 to 2013. He is now with the Tianjin Animal Sciences Institute as an Associate Investigator, in the study and application of reproduction bio-technology in domestic animals.

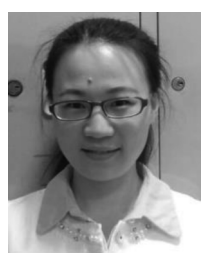

Yu Jin is working towards the M.S. degree in control theory and control engineering at the Institute of Robotics and Information System, Nankai University, Tianjin, China.

Her research interests include micro-manipulation and image processing.

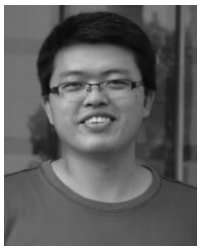

Yanding Qin received the B.Eng. and M.Sc. degrees in industrial design and the Ph.D. degree in mechanical engineering from Tianjin University, Tianjin, China, in 2005, 2007, and 2012, respectively.

From 2009 to 2010, he was a Visiting Scholar with the School of Mechanical Engineering, Purdue University, West Lafayette, IN, USA. From 2012 to 2013, he was a Postdoctoral Research Officer with the Robotics and Mechatronics Research Laboratory, Department of Mechanical and Aerospace Engineering, Monash University, Clayton, Australia. He is currently a Lecturer with the Institute of Robotics and Automatic Information System, Nankai University, Tianjin. His research interests include flexure-based mechanism, micro/nanomanipulation, hysteresis modeling and compensation, laser-based measurement, mechanical dynamics, 3D-bioprinting, and super-resolution microscopy.

Xin Zhao (M'12) received the B.S. degree from Nankai University, Tianjin, China, in 1991, the M.S. degree from Shenyang Institute of Automation, CAS, Shenyang, China, in 1994 , and the Ph.D. degree from Nankai University, in 1997, all in control theory and control engineering.

He joined the faculty at Nankai University in 1997. He is a Professor and Vice Dean ofthe College of Computer and Control Engineering. His research interests are in mico-nano manipulation and system, including micro manipulator, micro system and mathematical biology.